GEOFIZIKA VOL. 43 2026

DOI: https://dx.doi.org/10.15233/gfz.2026.43.5
Professional paper

Evaluation of iron-copper mineralisation around Avanos-Ozkonak (Nevsehir, Central Anatolia, Turkey) using satellite-based tectonic lineaments and surface temperature

Ramazan Demircioğlu

Department of Emergency Aid and Disaster Management, Faculty of Health Sciences, Aksaray University, 68100, Aksaray, Turkey

Received 7 August 2025, in final form 28 January 2026

This research focuses on Özkonak and the surrounding area in the Avanos district, investigating the relationship between tectonic lineaments and the formation of goethite and malachite mineralisation. The study aims to clarify how structural geological features influence the formation processes of these secondary minerals. Recent advances in satellite technology have greatly improved the effectiveness of remote sensing in mineral exploration. The study combined field surveys with Landsat-8 OLI/TIRS satellite imagery, processed using Geomatica, ENVI, and ArcGIS, to investigate the relationship between geological-tectonic lineaments and mineralisation patterns. The results indicate a strong correlation between mineralisation and tectonic lineaments, with significant concentrations of goethite and malachite mineralisation found to the west of Özkonak. This is particularly evident in areas characterised by imbricated thrust faults. These formations are likely to be secondary in the oxidation zone, suggesting the presence of primary sulphide deposits. The occurrence of mineralisation coincides with regions of significant tectonic lineaments, as shown by rose diagrams derived from both field and satellite data. The analysis revealed that the ore veins' position was N83°W/17°SW. The average orientation of the ore veins aligns with the N80-90°W and N30-50°E trending lineaments. In addition, a satellite-based surface temperature map indicates higher temperatures in the mineralised areas, which corresponds with the lineament maps. The results of this study could greatly enhance the exploration of primary sulphide deposits, which are the source of secondary mineralisation.

Keywords: Central Anatolia, Ozkonak, iron-copper mineralization, lineament, surface temperature.

1. Introduction

The study area is situated near the center of the Kırsehir Massif. To the north lies the Pontides, one of Turkey's tectonic units, while the Taurides are to

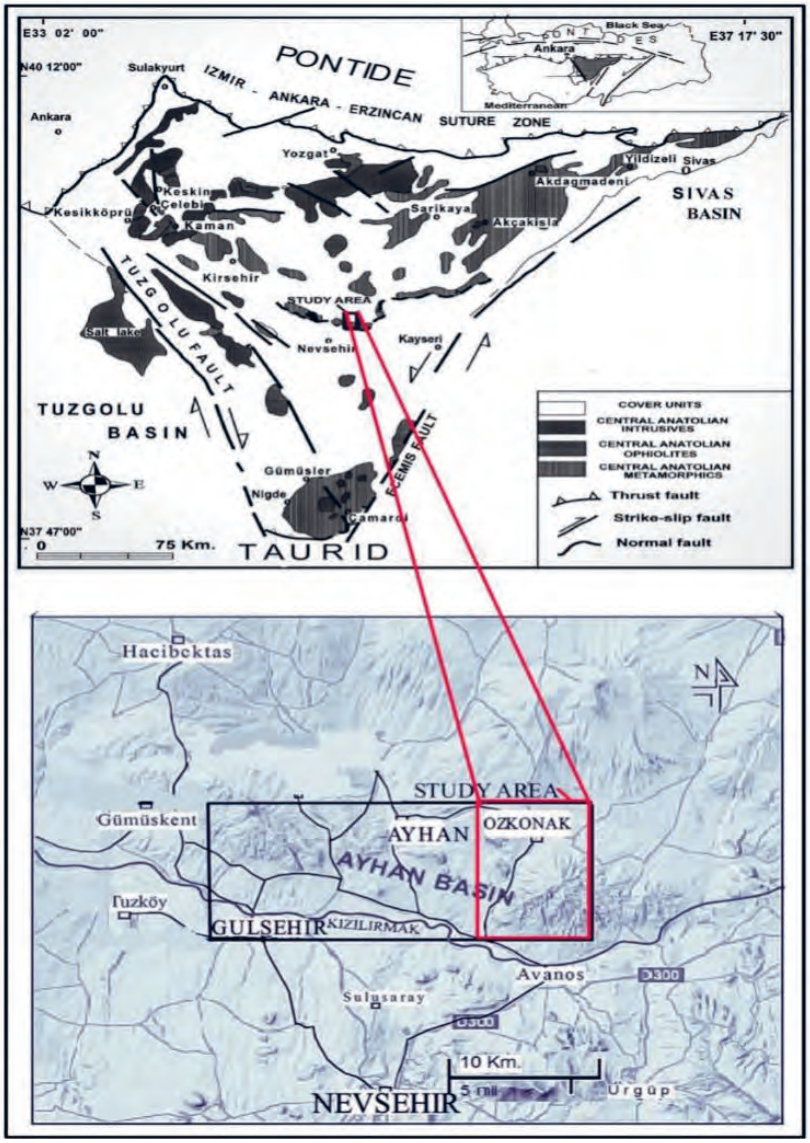


Figure 1. Map of the study area and its surroundings (modified from Kuşçu, 2001).

the south. The study area is located on the Kirsehir massif, north of Nevsehir province (Fig. 1).

Remote sensing is critical to mineral exploration today, and satellite imagery is commonly used. Lineaments identified by remote sensing from satellite imagery and aerial photography are categorised as either natural or man-made.

There have been some studies to determine this (Cracknell and Hayes, 1993; Jordan and Schott, 2005). Linear structures include the Great Wall of China, dams, roads, field boundaries, airport runways and irrigation canals. Remote sensing studies can detect tectonic lineaments such as faults, cracks and fold axes by combining satellite imagery with computer programs. There has been considerable research in this area. Some of these include (Osumeje et al., 2021; Tende et al., 2022). Lineaments derived from satellite imagery are also used in various engineering fields. Related studies have also been carried out (Sedrette, and Rebai, 2016; Mahdi and Haghighi, 2022). More recently, lineament determination studies have combined the use of ENVI, Arc-GIS, RockWorks and Geomatica (Ganguly and Mitran, 2016). There is a very important link between tectonic lineaments and source formation. Many studies have been carried out on this subject. Some examples are (Akbari and Haghighi, 2022; Goswami et al., 2022).

Remote sensing, satellite and aerial photography studies, and lineaments are very important in mineral exploration studies. During the 1980s, a remarkable increase in the use of satellites and the development of computer programs led to significant advances in the exploration of mineral deposits and their correlation with lineaments.

This interesting topic has been the focus of many studies; (Ilani et al., 1985; Maude, 1987; Good and De Wit, 1997). Since the turn of the millennium, there has been an even greater emphasis on the study of mineral deposits and their association with lineaments. Some of these are (Hill et al., 2002; Arian and Nouri, 2015; Arian and Reza, 2015; Chen et al., 2020; Barhoumi et al., 2021; El Galladi et al., 2022; Mahdi et al., 2022). Considerable geological research has been carried out in and around the study area. The first studies were mainly petrographic. Some of them are (Güleç, 1994; Kuşçu, 2001). Sedimentological studies have also been carried out in the basin. Some of them are, tectonic-structural geological studies; (Seymen, 1982; Koçyiğit and Doğan, 2016; Demircioğlu, 2014; Eldert et al., 2014). There are no studies on mineral deposits and mineralisation in Ozkonak (study area). This study aims to contribute to future detailed mineral exploration studies in this area, which is considered to have significant potential in terms of mineralisation.This research attempted to identify the link between iron-copper mineralization and tectonic linearity as indicated by field observations. This study will make an important contribution to future mineral exploration studies.

In this study, unlike previous studies, both field- and satellite-based studies were evaluated together. The aim was to determine the relationship between the areas where mineralisation was identified and tectonic linear features such as faults and fractures. Studies on this subject have also been conducted in different regions of the world. Some of these are (Ananaba and Ajakaıye, 1987; Hill et al., 2002; Arian and Nouri, 2015; Alaoui et al., 2025).

2. Geological Setting

2.1. Geological features

The Anatolian plate lies between the African and Eurasian plates. In this region, folded mountain belts, fault lines and volcanic activity have developed.

In the study area, the syenitoid (Mesozoic – Late Cretaceous) intruded into the metamorphic rocks of the Kırşehir Massif as a result of the subduction of the oceanic plate of the Inner Tauride Ocean under the Kırşehir Massif and partial melting of the subducting plate. Then, andesitic magmatism formed and cut the syenites (Fig. 2a).

The extensional tectonic regime continued until the Middle Eocene. In the post-Lutesian period, the compressional regime started and continued until the Late Miocene. During this period, the Late Palaeocene-Middle Eocene aged sedimentary units formed in terrestrial and marine environments in the Ayhan basin underwent two-stage deformation (D1-D2) and three-stage folding (F1, F2, and F3). In the D1-stage deformation, southwest-northeast directional compression occurred (Fig. 2b).

In this stage, imbricate thrust, reverse and strike-slip faults were formed (Demircioğlu, 2014). Along the planes of these thrust faults, goethite, hematite,

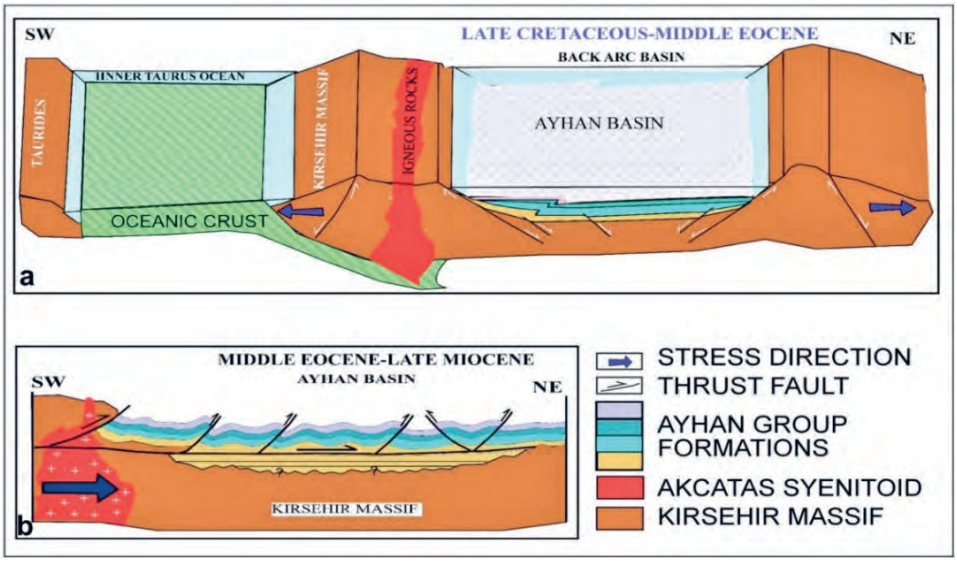


Figure 2. a) Geodynamic evolution of the Ayhan basin, Late Cretaceous to Middle Eocene and b) Geodynamic evolution of the Ayhan basin, Middle Eocene to Late Miocene (modified from; Demircioğlu, 2014).

and malachite were formed as secondary mineralization in the form of veins. Then, in the second deformation stage (D2), southeast-northwest directional compression occurred.

These basement units are unconformably overlain by sedimentary units of Late Palaeocene–Middle Eocene age (Fig. 3). The young-aged units of the study area are Middle Miocene-Pliocene-Quaternary-Holocene aged volcano sedimentary units. These units unconformably cover the underlying units.

2.2. Structural geological features

The researched region is situated in the Kirsehir massif (Fig. 1). The basement rocks are composed of metamorphic and igneous rocks from the Paleozoic-Mesozoic age, which are overlain unconformably by units from the Late Paleocene-Middle Eocene period (Fig. 3).

The Palaeocene-Lower-Middle Eocene-aged units experienced two deformation phases and three phases of folding, as indicated on the structural map (Fig. 3). However, the extensional regime during the Pliocene-Quaternary period prevented the younger units from undergoing any folding (Fig. 3). Tectonic lineaments are formed by the lines of fold axes, faults and fractures resulting from deformation (Demircioğlu, 2014).

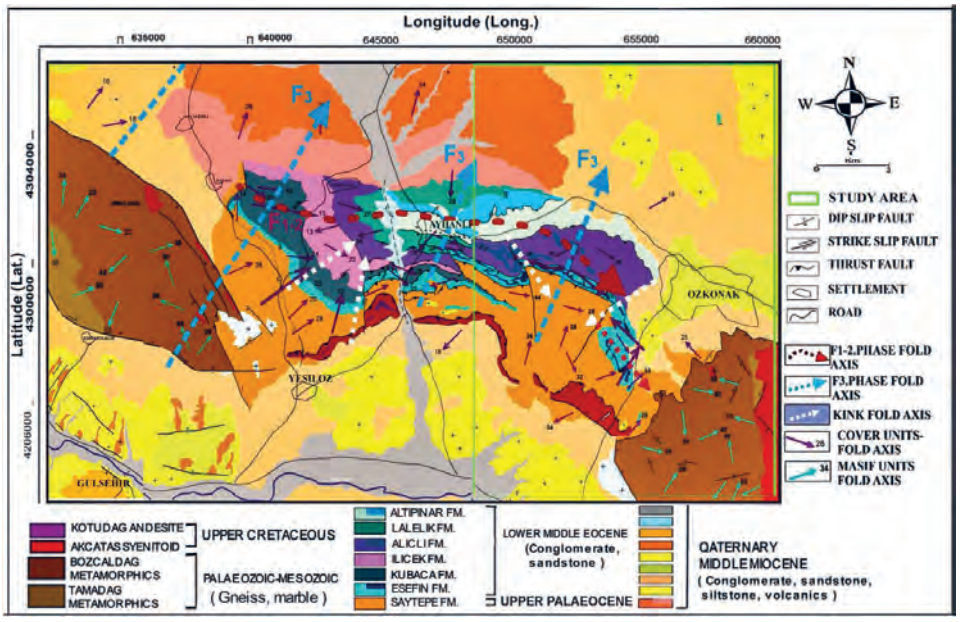


Figure 3. Geology map and structural features map of the study area (modified from Demircioğlu, 2014).

3. Materials and methods

3.1. Preparation of lineament maps

The research involved a comprehensive approach, beginning with field studies followed by the acquisition of satellite images. These findings were then combined with office studies. During the field studies, the Brunton compass was used to measure planar and linear structures and a geological map of the area was created. The measurements and structural elements were assessed to develop a structural geological map (Fig. 3). Notably, goethite and malachite mineralisations were discovered during the field studies. To create the lineament maps, a Landsat-8 OLI/TIRS satellite picture of the research region was downloaded from a reputable website (U.S. Geological Survey, 2023). The Landsat-8 image undergoes pre-processing in the ENVI (ENVI, 2018) and Geomatica (Geomatica, 2016) programs. We used the line module with the edge sharpening filter to produce the tectonic structure lineament map.

In this study, the parameters for lineament extraction and their threshold values proposed by Sedrette and Rebai (2016) were adopted and considered sufficient (Table 1). The filter radius (pixel value) specifies the number of pixels surrounding the central pixel that are included in the filter calculations. The edge gradient value is used in image processing and edge detection. The curve length value represents the length of a curve. The line fit error values are numbers that show how far off the predicted line are from the actual data points. The angular difference value indicates the difference between two angles. The connection distance value indicates how the connections provided by the connection value are shared.

The image was then processed in the Arc-GIS (ArcGIS Pro, 2024) environment, resulting in the creation of lineament maps. You can find this process outlined in the flowchart for generating lineament maps and Rose diagrams (Fig. 4). The Landsat-8 image undergoes pre-processing in the ENVI and Geomatica programs. To create the linearity map of tectonic structures, we utilized the line module and applied the edge sharpening filter. In the realm of work, threshold values essential for ensuring proper assessment have been established. These threshold values may differ based on the specific objectives and particulars of the work.

Table 1. Parameters used for lineament extraction (after Sedrette and Rebai, 2016).

Edge Sharpening Filter	
Threshold values:	
Filter Radius in Pixel Value	10
The threshold for edge gradient value	100
Threshold curve length value	30
Threshold for line fitting error values	3
Threshold for angular difference values	30
Threshold for Linking Distance Value	20

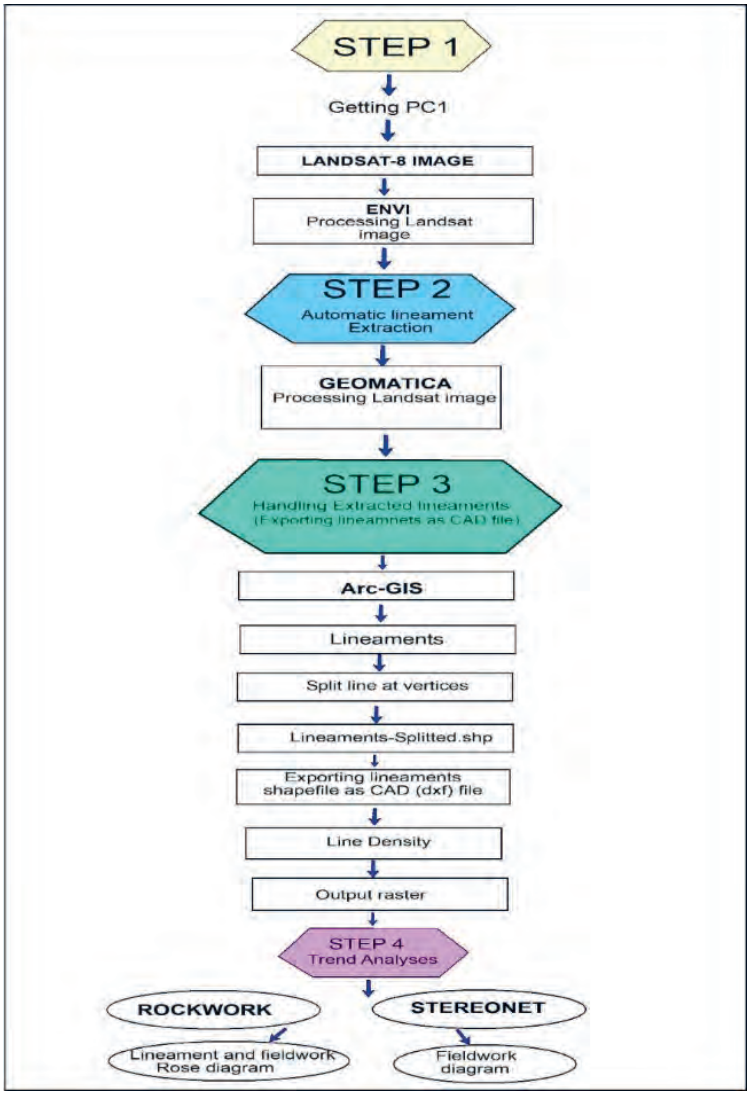


Figure 4. Flowchart for creating a lineament map (modified from Demircioğlu et al. 2024).

Lineament maps were created with satellite images and data obtained from field studies. The relationships between the lineaments and mineralisations were determined.

To create the lineament map, we utilised various programs, including Landsat-8 satellite images, the ENVI program, ArcGIS, Geomatica, and RockWorks (RockWorks, 2019). We generated density maps of the lineaments and analysed field measurements using the Stereonet 3.02 program (Allmendinger et al.,

2013). The measurements of goethite and malachite veins collected during the fieldwork were also analysed with this program. Finally, we compared data obtained from satellite images and field research to gain a deeper understanding of mineralization. During our field studies, we took measurements of the goethite and malachite veins, which were evaluated using the Stereonet 3.02 program. The data gathered from satellite images and field studies were then used to construct lineament maps and assess the relationships between mineralisation.

A comprehensive map of Earth's surface features, called lineaments, was created using advanced satellite imagery from Landsat-8, alongside top-of-the-line software such as ENVI, ArcGis, Geomatica, and RockWorks. The lineaments were plotted with meticulous density, and precise measurements were taken during field studies using the Stereonet 3.02 program. This same program was also utilized to analyze goethite and malachite vein measurements collected during field studies. By carefully comparing satellite imagery data and field study data, we were able to generate highly accurate lineament maps and establish valuable connections between mineralization.

3.2. Satellite-based- surface temperature map

This study employed Landsat-8 OLI/TIRS data from the 2023/07/14 Landsat series to determine ground surface temperature (pictures of Ozkonak are dated 2023/08/12 for K33B4 plots). Landsat is the oldest known medium-resolution multispectral earth observation satellite. It delivers regular (every 16 days) imaging in a variety of band ranges, including visible, infrared, and thermal (Alkan et al., 2017).

The picture with a cloudiness rate of 0% was selected to minimise the cloud effects on the calculated surface temperature.

3.3. Calculation of Earth Surface Temperatures

Automatic radiometric and geometric corrections were performed on the Level 2 images used in the study. The spectral radiance ($L\lambda$) values measured by the satellite were obtained by converting the digital number (DN) values of the pixels in the image. This process was carried out using Eqs, 1 and 2 (Alkan et al., 2017).

$$L_\lambda = gain \cdot DN + bias \tag{1}$$

$$L_\lambda = M_L Q_{cal} + A_L \tag{2}$$

where

L_λ: spectral radiance ($Wm^{-2} sr^{-1} \mu m^{-1}$)
M_L: band-specific multiplicative rescaling factor
A_L: band-specific scaling summation factor
Q_{cal}: quantized and calibrated standard pixel values (DN).

The conversion of the calculated spectral radiance value into a brightness temperature is necessary. Eq. 3 (Url-1) illustrates the formula required for this conversion.

$$T = \frac{K_2}{\ln\left(\frac{K_1}{L_\lambda} + 1\right)} \tag{3}$$

where

T: Brightness temperature reaching the satellite (K)
L_λ: spectral radiance ($Wm^{-2}\,sr^{-1}\,\mu m^{-1}$)
K_1, K_2: band-specific thermal conversion constants

The surface temperature calculated in Kelvin units was converted to Celsius units. The calculation steps for the ground surface temperature were carried out in QGIS 3.34 software. The lack of forest and vegetation cover in the study area influences surface temperature, impacting evaporation and transpiration (Alkan et al., 2017).

4. Results

4.1. Automatic lineament map

A detailed map of the Earth's surface features, called lineaments, was expertly crafted using advanced satellite imagery from Landsat-8, along with powerful software like ENVI, ArcGis, Geomatica, and RockWorks (Fig. 5). The den-

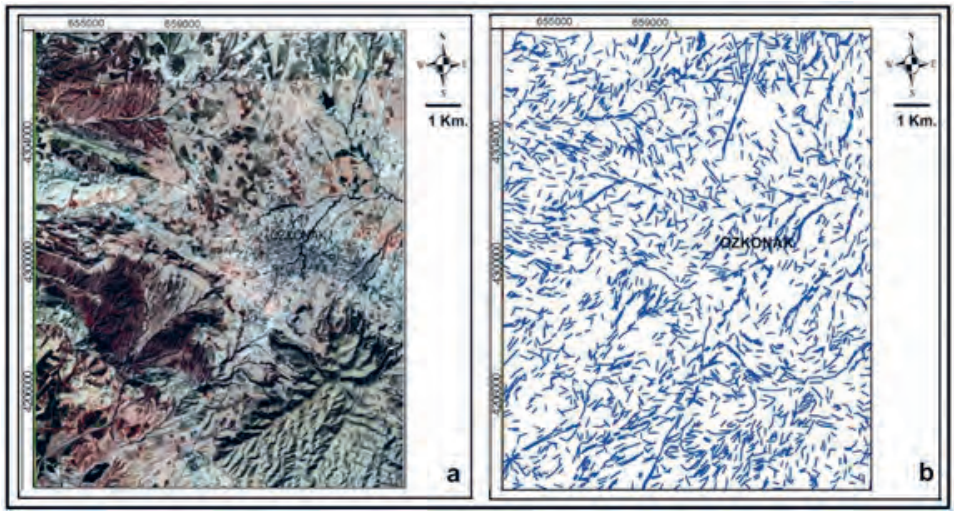


Figure 5. (a) A Landsat-8 satellite image of the research region. (b) Lineament of the satellite image.

sity of these lineaments was meticulously plotted, and precise measurements were taken with the Stereonet 3.02 program during field studies. Additionally, the Stereonet 3.02 program was employed to analyze the goethite and malachite vein measurements gathered in the field. Accurate lineament maps have been developed by comparing satellite imagery and fieldwork data, revealing significant relationships between mineralization.

To assess the geological structures in the vicinity of Ozkonak, a line map and a satellite image were integrated and overlaid. The resulting image enabled the identification of linearity patterns in and around Ozkonak, as depicted in Fig. 6a. A density map of the identified lineaments was then generated, as presented in Fig. 6b. Additionally, automatic lineament detection algorithms were employed to create density and lineament maps, as shown in Fig. 6c. These analytical outputs provide valuable insights into the geological features of the

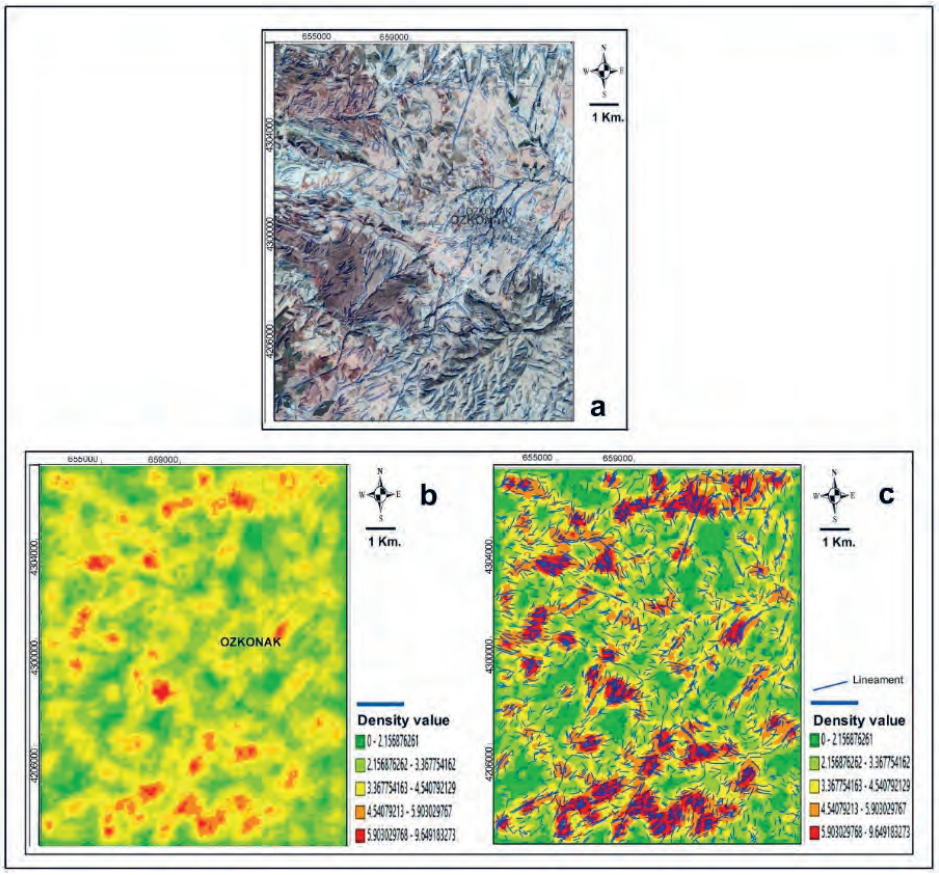


Figure 6. a) A satellite-lineament map of Ozkonak and its region. b) Lineament density map. c) Lineament density map with lineament.

area. Morphological lines identified in the field studies as resulting from erosion were excluded from the tectonic lineaments.

Structures such as faults and fractures are seen as tectonic lineaments. The morphology of the area may form linear lines due to erosion. The morphological lineaments identified in the field were kept separate from the tectonic lineaments.

4.2. Faults and fractures forming lineaments in the terrain

Mineralisation has been identified along the thrust faults to the west of Ozkonak (Fig. 3). However, this study focuses on the area with the most intense mineralization.

After the Middle Eocene in the Ayhan basin, the beginning of the compressional tectonic regime (D1 deformation stage) led to the development of nested reverse and thrust faults. Primary ore is thought to have been transported to these thrust planes where it underwent oxidation and secondarily mineralization Hydrothermal fluids probably interacted with and enriched the underlying sulphide deposits (such as pyrite, chalcopyrite and bornite) and caused the formation of secondary minerals such as goethite and malachite along the fault planes. Further investigation of the primary sulphide deposits is recommended.

To create lineament maps of the study area (Ozkonak) and to determine the relationships between them and mineralisation, data were collected from both satellite images and field studies. Lineament maps of Ozkonak and its region were created. Then, density maps of the obtained lineaments were prepared. Measurements of ore veins measured in the field were also analysed using Stereonet 3.02 software.

Fault orientations and fracture orientations are prominent geological features formed by the polyphase deformation of metamorphic rocks within a massif. This deformation leads to significant fracturing and faulting in these rocks. In the Ayhan basin, even though the rocks have undergone less deformation, they have still experienced fracturing and faulting during the Late Palaeocene-Middle Eocene period. These structures have played a crucial role in the formation of mineral deposits and the creation of critical discontinuity surfaces.

To analyze these structures, RockWorks software was used to generate rose diagrams that display %L (Number of total lineaments) and %N (length of total lineaments population), highlighting automatic linearities. The diagrams illustrate a widespread distribution of lineaments in all directions, with the most prominent orientations being N40°–50E, N30°–40E, N50°–60E, N80°–90W, N70°–80W, and N60°–70W (as shown in Fig. 7a,b). During fieldwork, measurements of the goethite and malachite veins were evaluated in stereographic projection (Fig. 7c). The analysis revealed that the ore veins' position was N83°NW/17°SW. The average orientation of the ore veins aligns with the N80°–90°W and N30°–50°E trending lineaments (Fig.7c).

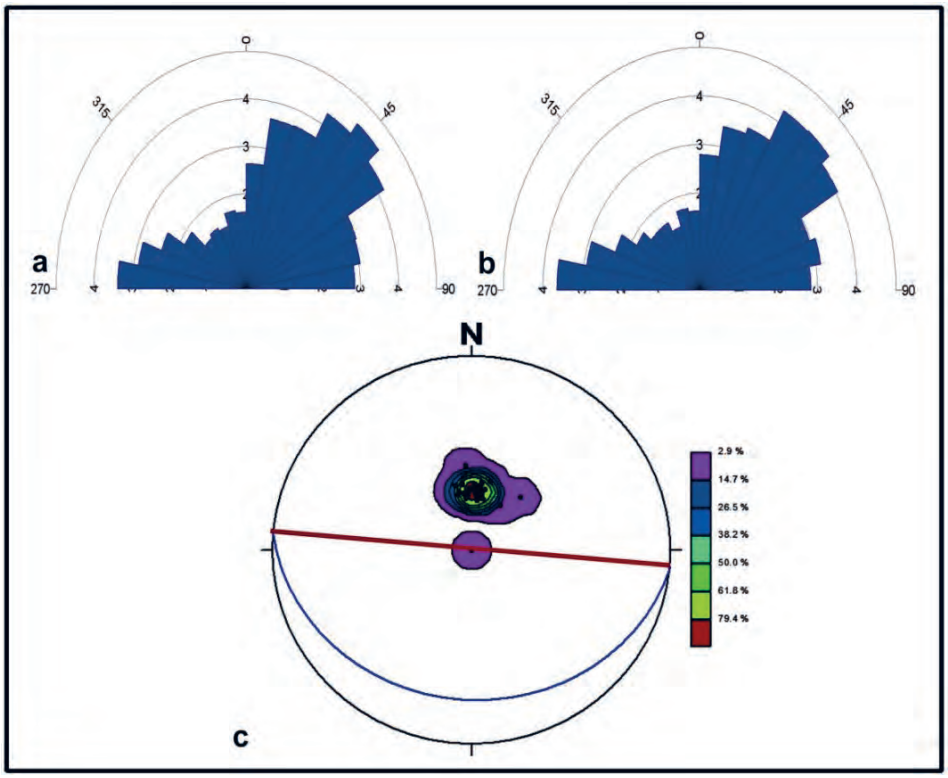


Figure 7. a) %L: Rose diagram of the Number of total lineaments. b) %N: Rose diagram of the length of total lineaments population. c) Pole-point contour diagram of the gutite and malachite veins.

The study area is characterized by a high density of faults and fractures, particularly in the mineralized regions (Fig. 8a).

Mineralizations are located along the thrust fault planes (Fig. 8b). Goethite veins were formed within the discontinuities in the fault planes (Fig. 8 c, d and e). Similarly, malachite veins were formed in the discontinuities in the thrust fault planes (Fig. 8 f,g).

Finally, in order to better understand the mineralisation, data collected from satellite photographs and fieldworks were compared. According to these studies, it is seen that the satellite-based data and the data obtained by field surveys are largely compatible.

4.3. Mineralization and its relationship with tectonic lineaments and surface temperature

The identification of tectonic lineaments in this study refers to the analysis of fold axes, faults, and fractures. The researcher was able to locate these linea-

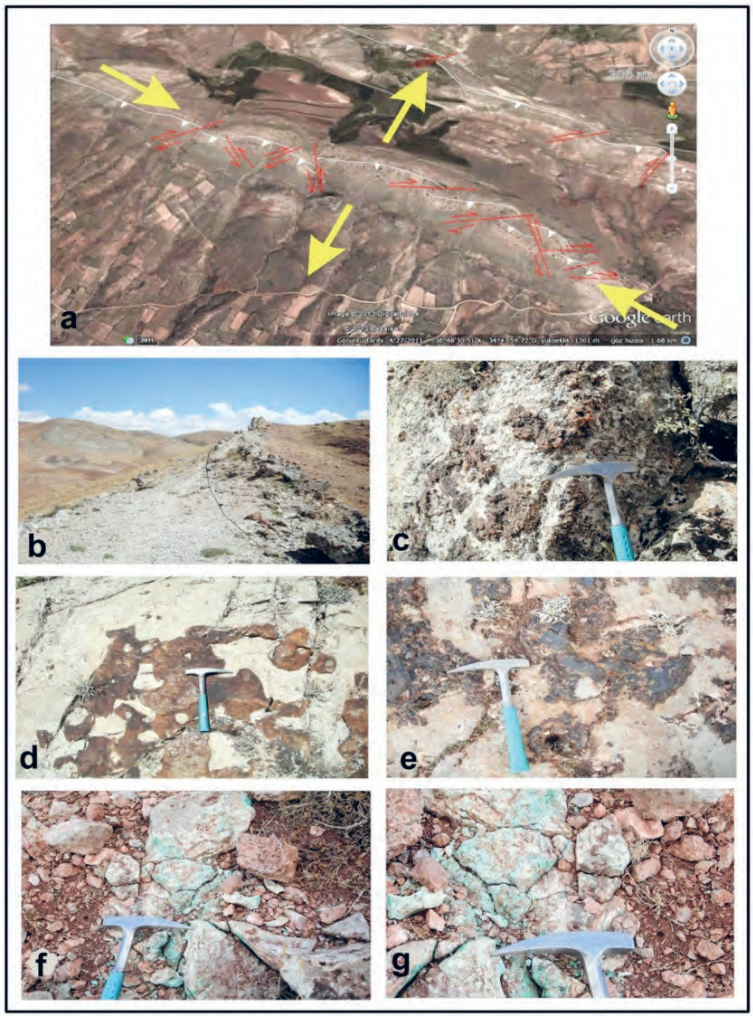


Figure 8. a) Google Earth image of faulting in mineralization zones. b) Thrust fault plane and goethite mineralisation. c), d) and e) Goethite mineralization on thrust planes. f) and g) Malachite mineralization on thrust planes.

ments in the study area by analysing satellite images and conducting field research. Mineralisations were found to be concentrated in areas with dense and consecutive thrust faults, particularly in the western part of Ozkonak. The area is characterised by frequent occurrences of strike-slip and thrust faults resulting from the D1 stage deformation, which were later intersected by the D2 stage. The southeast-northwest directional thrust faults were formed under the influence of the compressive regime. The observed shearing in the ore veins is re-

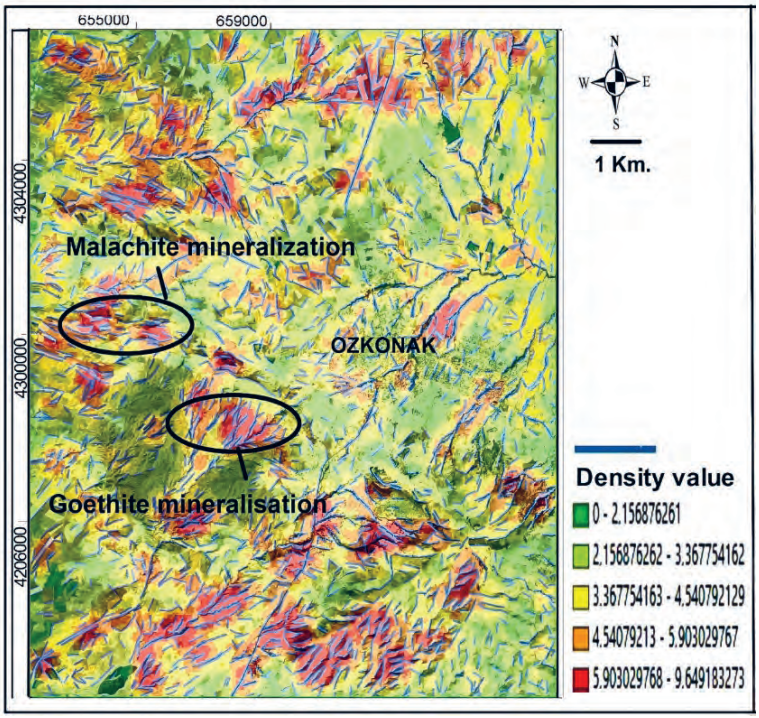


Figure 9. Map of the study area's lineament density and mineralisation.

lated to the faults in the area. The most intense mineralisation occurs near fault intersections, essential for water resources and geothermal formation.

The lineament density and mineralisation map of the study area supports this observation (Fig. 9). An ongoing study is being conducted to better understand the link between tectonic lineaments and mineral occurrences (Fig. 9). Since the study area is also located in an area of intense young volcanism, a map of lineaments and surface temperature can be very useful.

The high-temperature values in the satellite-based surface temperature map are consistent with the tectonic lineaments, particularly in the areas with intense tectonic lineaments and ore zones (Fig. 10).

5. Conclusions And Discussions

The aim of this study was to investigate the relationship between goethite and malachite mineralisation discovered during fieldwork and the lineaments identified through satellite imagery. Researchers analysed a Landsat-8 OLI/TIRS satellite image-sourced web to explore the connection between the observed

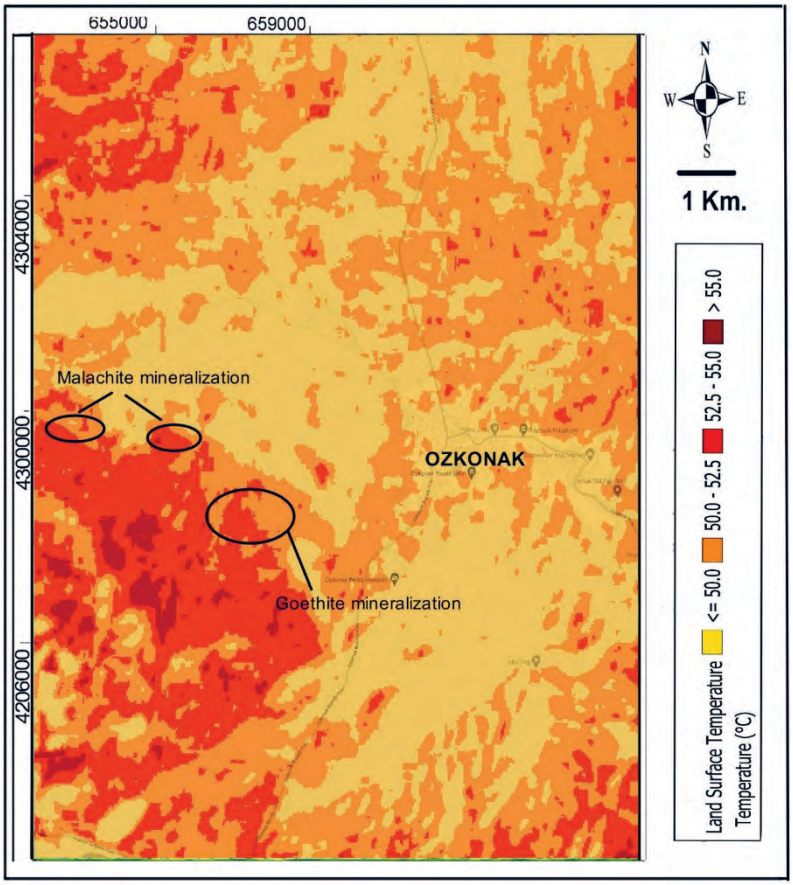


Figure 10. Map of the study area surface temperature map and mineralisation.

lineations during the field study and mineral formation. The results indicated a significant correlation between mineralisation and tectonic lineaments, particularly in the western region of Ozkonak, where substantial deposits of goethite and malachite, along with secondary mineral formations, were found in the oxidation zone near the surface. The observed formations are likely associated with tectonic lineaments. The secondary mineralisation of goethite and malachite is believed to have been mobilised by hydrothermal fluids originating from underlying sulphur deposits, which constitute the primary mineralisation. This mobilisation occurred along thrust fault planes, where the minerals subsequently crystallised as vein deposits.

The lineament map of the study area revealed significant geological features, including imbricate thrust faults and several smaller directional thrust faults

that intersect with these imbricate faults. In contrast, the younger sedimentary units to the north displayed minimal signs of tectonic activity, with few observable lineaments and no indications of mineralization. Rose diagrams for these lineaments were created using the automated lineament mapping feature of the RockWorks program. Due to the polyphase deformation history in the surveyed area, lineaments appeared in various orientations.

The most intense lineament orientations are N40°–50°E, N30°–40°E, N50°–60°E and N80°–90°W, N70°–80°W, and N60°–70°W. After conducting field measurements and evaluating the data in stereographic projection, it was determined that the goethite and malachite veins have a vein position of N83°W/17°SW. The direction of the ore veins aligns with the N80°–90°W trending lineaments. In the study area, the highest concentration of mineralisation is situated to the west of Ozkonak. The presence of goethite and malachite suggests a significant potential for mineral exploration in this region. Further geological assessments are warranted to assess the extent and viability of mineral deposits.

Satellite-based land surface temperature (LST) maps vary depending on numerous natural and anthropogenic factors. Seasons, land cover, and humidity levels may influence these variations. The entire study area is relatively barren in terms of vegetation cover. In this respect, it possesses a homogeneous structure.

Analysis of the satellite surface temperature map shows that areas containing goethite and malachite mineralisation generally have higher surface temperatures. Furthermore, there appears to be an approximate correlation between the density of tectonic lines and surface temperature; areas with dense fault lines generally have high surface temperatures. These minerals may serve as indicators of primary mineral deposits and suggest that further exploration work is needed. When conducting studies related to surface temperature in particular, regional climate factors and vegetation cover, as well as factors such as soil moisture content, should be taken into account.

Acknowledgements: I would like to thank Efdal Kaya for his support. I would also like to thank the journal editors and reviewers for their contributions to the preparation of this article.

Data availability statement: The author may provide the data under request.

References

Akbari, M. and Haghighi A.T. (2022): Satellite-based agricultural water consumption assessment in the ungauged and transboundary Helmand Basin between Iran and Afghanistan, *Remote Sens. Lett.,* 13, 1236–1248, https://doi.org/10.1080/2150704X.2022.2142074.

Alkan, A., Adıgüzel, F. and Kaya, E. (2017): The Importance of Green Places in Decreasing the Urban Temperature in Batman, *Coğr. Derg.,* 34, 62-76.

Alaoui, I.M., Akhssas, A., Bahi, A., Ibouh, H, Himyari, S.M., Khebbi, H. and Sbabou, F. Z. (2025): Tectonic lineament mapping and identification of copper alteration minerals using PRISMA and

Sentinel-2A satellite imagery in Alma inlier and Fouanou syncline (western Anti-Atlas, Morocco), *Sci. Afr.,* 30, e02961, https://doi.org/10.1016/j.sciaf.2025.e02961.

Allmendinger, R. W., Cardozo, N., and Fisher, D. (2013*): Structural geology algorithms: Vectors and tensors*. Cambridge University Press, 289 pp.

Ananaba, S. E., and Ajakaıye, D. E. (1987): Evidence of tectonic control of mineralization in Nigeria from lineament density analysis A Landsat-study, Int. J. Remote Sens, 8(10), 1445–1453, https://doi.org/10.1080/01431168708954788.

ArcGIS Pro (2024): Esri Inc., version 14.1, Environmental Systems Research Institute, Redlands, CA, USA. Available at: https://www.esri.com.

Arian, M. and Nouri, R. (2015): Lineament Tectonics and Mineralization in Tarom Area, North Iran, Open J. Geol., 5, 115-125, https://doi.org/10.4236/ojg.2015.53011.

Barhoumi, A., Belkhiria, W., Ayari, J., Hatira, N., Braham, A. and Dhaha F. (2021): Tectonic controls on the salt diapir-related Mississippi Valley-type lead-zinc mineralization of Fej El Adoum ore deposit (Northern Tunisian Atlas): Constraints from detailed gravity and drill hole data, J. Afr. Earth Sci., 181, 104237, https://doi.org/10.1016/j.jafrearsci.2021.104237.

Chen, Q., Zhao, Z., Zhou, J., Zeng, M., Xia, J., Sun, T. and Zhao, X. (2020): New Insights into the Pulang Porphyry Copper Deposit in Southwest China: Indication of Alteration Minerals Detected Using ASTER and WorldView-3 Data, Remote Sens., 13(14), 2798, https://doi.org/10.3390/rs13142798.

Cracknell, A.P. and Hayes, L.W.B. (1993): Introduction to Remote Sensing. Taylor & Francis, London, 352 pp.

Demircioğlu, R. (2014): The geology and structural characteristics of the Kırşehir Massif and its cover units around Gülşehir-Özkonak (Nevşehir). PhD Thesis, S.Ü. Institute of Science, Konya, 232 pp.

Demircioğlu, R., Eren, Y., Coskuner, B. (2024): The Extraction and Structural Analysis of Lineaments Around Gülsehir (Nev¸sehir) Using GIS Methods, *Geofísica Int.,* **63**, 1175–1191, https://doi.org/10.22201/igeof.2954436xe.2024.63.4.1725.

ElGalladi, A., Araffa, S., Mekkawi, M. and Abd-AlHai, M. (2022): Exploring mineralization zones using remote sensing and aeromagnetic data, West Allaqi Area, Eastern Desert, Egypt, *Egypt. J. Remote Sens. Space Sci,* 25(2), 417-433, https://doi.org/10.1016/j.ejrs.2022.03.007.

ENVI (2018): NV5 Geospatial Solutions, version 5.1, Boulder, CO, USA.

Ganguly, K. and Mitran, T. (2016): Delineation and assessment of Central Indian Suture through lineament extraction approach using Remote Sensing and Geographic Information System, *Geocarto Int,* 31(3), 308-327, https://doi.org/10.1080/10106049.2015.1047417.

Good, N. and De Wit, M.J. (1997): The Thabazimbi-Murchison lineament of the Kaapvaal craton, South Africa: 2700 Ma of episodic deformation, *J. Geol. Soc.,* 154(1), 93-97.

Goswami, S., Rai, A.K. and Tripathy, S. (2022): Re-visiting Geothermal Fluid Circulation, Reservoir Depth and Temperature of Geothermal Springs of India, *J. Hydrol,* 612, 128131, https://doi.org/10.1016/j.jhydrol.2022.128131.

Güleç, N. (1994): Rb-Sr isotope data from the Ağaçören Granitoid (East of Tuz Gölü): geochronological and genetical implications, Turk. J. Earth Sci, 3, 39-43.

Hill, K.C., Kendrick, R.D., Crowhurst, P.V. and Gow, P.A. (2002): Copper–gold mineralisation in New Guinea: Tectonics, lineaments, thermochronology and structure, *Aust. J. Earth Sci.*, 49(4), 737-752, https://doi.org/10.1046/j.1440-0952.2002.00944.x.

Ilani, S., Kronfeld, J. and Flexer, A. (1985): Iron-rich veins related to structural lineaments, and the search for base metals in Israel, *J. Geochem. Explor.,* 24(2), 197-206, https://doi.org/10.1016/0375-6742(85)90045-7.

Jordan, G. and Schott, B. (2005): Application of wavelet analysis to the study of the spatial pattern of morphotectonic lineaments in digital terrain models. A case study, *Remote Sens. Environ.,* 94(1), 31-38, https://doi.org/10.1016/j.rse.2004.08.013.

Koçyiğit, A. and Doğan, U. (2016): The strike-slip neotectonic regime and related structures in the Cappadocia region: a case study in the Salanda basin, Central Anatolia, Turkey, *Turk. J. Earth Sci.,* 25(5), 393-417, https://doi.org/10.3906/yer-1512-9.

Kuşçu, I. (2001): Geochemistry and mineralogy of the skarns in the Celebi district, Kırıkkale, Turkey, *Turk. J. Earth Sci.,* 10, 121-132.

Mahdi, A. M., Eldosouky, A. M., El Khateeb, S. O., Youssef, A. M. and Saad, A. A. (2022): Integration of remote sensing and geophysical data for the extraction of hydrothermal alteration zones and lineaments; Gabal Shilman basement area, Southeastern Desert, Egypt, *J. Afr. Earth Sci.,* 194, 104640, https://doi.org/10.1016/j.jafrearsci.2022.104640.

Maude, R. (1987): Lineaments in enhanced Landsat images from a portion of west Wales, *Geol. J.,* 22, 107-118.

Osumeje, J. O., Onıku, A. S. and Meludu, O. C. (2021): Analysis Of Lineament Map Of Part Of Maru Schist Belt, Northwest, Nigeria And Its Implicatıon For Mineral Exploration, *Fudma J. Sci.,* 5(3), 355-362, https://doi.org/10.33003/fjs-2021-0503-721.

Geomatica (2016): PCI Geomatics version 2016, Markham, ON, Canada.

RockWorks (2019): RockWare Inc., version 2019.6.11., Golden, CO, USA.

Sedrette, S. and Rebai, N. (2016): Automatic extraction of lineaments from Landsat Etm+ images and their structural interpretation: Case Study in Nefza region (North West of Tunisia), *J. Res. Environ. Earth Sci,* 4, 139-145.

United States Geological Survey (2023): Landsat 8 OLI/TIRS Collection 2 Level-1, U.S. Geological Survey, https://doi.org/10.5066/P9OGBGM6.

SAŽETAK

Procjena željezno-bakrene mineralizacije u području Avanos – Ozkonak (Nevşehir, Središnja Anadolija, Turska) na osnovi strukturnih lineamenata i temperature površine određenih iz satelitskih snimaka

Ramazan Demircioğlu

Istraživanje je usmjereno na područje Özkonaka i njegove okolice u okrugu Avanos te ispituje povezanost između strukturnih lineamenata i formiranja mineralizacije getita i malahita. Cilj rada je razjasniti na koji način strukturno-geološke značajke utječu na procese nastanka ovih sekundarnih minerala. Nedavni napredak u satelitskoj tehnologiji znatno je unaprijedio učinkovitost daljinskih istraživanja u istraživanju mineralnih sirovina. U radu su kombinirana terenska istraživanja sa satelitskim snimkama Landsat-8 OLI/TIRS, obrađenima u programima Geomatica, ENVI i ArcGIS, kako bi se ispitala povezanost između strukturnih lineamenata i obrazaca mineralizacije. Rezultati ukazuju na snažnu korelaciju između mineralizacije i strukturnih lineamenata, pri čemu su značajne koncentracije mineralizacije getita i malahita utvrđene zapadno od Özkonaka. To je osobito izraženo u područjima obilježenima imbriciranim navlačnim rasjedima. Ove su tvorevine vjerojatno sekundarnog podrijetla u zoni oksidacije, što upućuje na prisutnost primarnih sulfidnih ležišta. Pojava mineralizacije podudara se s područjima izraženih strukturnih lineamenata, što potvrđuju rozetni dijagrami dobiveni iz terenskih i satelitskih podataka. Analiza je pokazala da je položaj rudnih žila N83°W/17°SW. Prosječna orijentacija rudnih žila podudara se s lineamentima smjera N80–90°W i N30–50°E. Dodatno, satelitski snimak temperature površine pokazuje povišene temperature

u mineraliziranim područjima, što je u skladu s kartama lineamenata. Rezultati ovog istraživanja mogu značajno pridonijeti istraživanju primarnih sulfidnih ležišta, koja predstavljaju izvor sekundarne mineralizacije.

Ključne riječi: Središnja Anatolija, Özkonak, željezno-bakrena mineralizacija, lineament, temperatura površine

Corresponding author's address: Ramazan Demircioğlu, Department of Emergency Aid and Disaster Management, Faculty of Health Sciences, Aksaray University, 68100, Aksaray, Turkey. email: ra.demircioglu@gmail.com

This work is licensed under a Creative Commons Attribution-NonCommercial 4.0 International License.